J Mater Sci (2008) 43:2222–2228
DOI 10.1007/s10853-007-2038-3

Hydrothermal/autoclave synthesis of AlPO-5: a prototype space/time study of crystallisation gradients

Vesna Middelkoop · Simon D. M. Jacques · Matthew G. O'Brien · Andrew M. Beale · Paul Barnes

Received: 24 November 2006 / Accepted: 20 July 2007 / Published online: 29 November 2007

Abstract TEDDI (tomographic energy dispersive diffraction imaging) has been used for in situ time-resolved studies of hydrothermal synthesis of Ge doped AlPO-5. The data for three different levels of Ge doping into AlPO-5 system are presented. Two pathways are observed, the simplest being a direct formation of ALPO-5 accompanied by simultaneous GeO_2 dissolution in the bulk gel, plus a variation in which ALPO-5 acts as an intermediate in the formation of ALPO-18, a related framework structure. The TEDDI approach is able to show that these synthesis pathways and kinetics vary significantly with depth inside the synthesis vessel and possible explanations for this are discussed.

Introduction

Hydrothermal/autoclave crystallisation is a common tool for batch synthesis and novel material design. Since autoclaves need to be sealed vessels, made from pressure/temperature-withstanding materials, a direct knowledge of hydrothermal *kinetics* and *synthesis pathways* requires the more demanding use of in situ probes that can monitor the reaction chemistry actually taking place inside the autoclave vessel. In the case of a "diffraction probe" this essentially requires the penetrating properties of either neutrons or high energy X-rays to "illuminate" the interior of the autoclave vessel. This idea started out in the early 1990's through the availability of neutron [1] and synchrotron X-ray [2, 3] sources and has been subsequently used to great effect, particularly with energy-dispersive (EDD) [4–6] and angle-scanning (ASD) [7, 8] X-ray diffraction modes. However such in situ studies have not dwelt on the spatial aspects of hydrothermal/autoclave synthesis, relying on the collection of time-resolved diffraction data from a single point or volume in the hydrothermal mix within the vessel. A recent study by Hooper et al. [9] has challenged this approach by considering the possibility of there being variations in reaction kinetics across the confines of the autoclave cell; in fact this study deliberately sought situations, such as substrate- or seed-assisted zeolite membrane growth, where crystallisation gradients might be favoured and this was indeed found to be the case. The emergence of *TEDDI* [10, 11] raises the prospect of re-examining many of the in situ studies cited in the literature to ascertain whether their assumption of "homogeneous kinetics" is really valid. Such a challenge requires adequate resolution in both the time and space domains, and so the tomographic configuration has had to be restricted to one-dimensional (vertical) scanning only. Following on from this, the long-term aim is to map growth-kinetics *gradients* for a range of materials synthesis with a view to feeding back this information into the design of synthesis cells.

V. Middelkoop (✉) · S. D. M. Jacques · P. Barnes
Materials Chemistry Centre, Department of Chemistry,
University College London, 20 Gordon Street, WC1H 0AJ,
London, UK
e-mail: v.middelkoop@ucl.ac.uk

V. Middelkoop · S. D. M. Jacques · P. Barnes
School of Crystallography, Birkbeck College,
University of London, Malet Street, WC1E 7HX, London, UK

M. G. O'Brien
Davy Faraday Research Laboratory, The Royal Institution,
21 Albemarle Street, W1S 4BS, London, UK

A. M. Beale
Department of Chemistry, Utrecht University,
Sorbonnelaan 14-16, 3584 CA, Utrecht, The Netherlands

The synthesis of the alumino-phosphate zeotype AlPO-5 was chosen as a model system to study since its metal related analogues have been amongst the most researched aluminophosphate microporous materials. AlPO-5 has the AFI framework-type structure which consists of open one-dimensional channels with 0.73 nm wide pores and overall framework neutrality. The simplicity of AlPO-5 synthesis makes it suitable for use in shape-selective catalysis, separation technology, in non-linear optics [12] and in novel applications such as hosts for the smallest carbon nanotubes [13]. Also various dopants can be introduced into the AlPO-5 framework and these can alter its catalytic performances and promote related framework structures, e.g. AlPO-18 (AEI type structure) and AlPO-34 (CHA type structure), as previously observed by others [14–17].

Methodology

TEDDI

Synchrotron-based *TEDDI* (tomographic energy dispersive diffraction imaging) has been developed [9–11, 18] as a means of non-destructively imaging the structural and chemical content of bulk systems such as large (∼centimetres) dense objects and intrusive materials science apparatus. The degree of penetration required is achieved through the use of intense hard white X-ray beams as produced by second/third generation synchrotron wiggler (magnet) devices. Each volume element within a selected region inside an object is successively illuminated by a highly reduced incident X-ray beam (typical cross section $\sim 25 \times 25$ μm^2 to 1×1 mm^2) and the intersection of this beam with the diffracted beam, that passes through the post-sample collimator into the detectors, defines the active volume element currently under interrogation (Fig. 1). Many such volume elements (typically 10^{-2} to 10 mm^3 in size) are visited by intelligent 1D-, 2D- or 3D-scanning of the sample through the X-ray beam and collecting the X-ray signal from each location by means of an energy-dispersive detector. This signal contains the diffraction pattern, and any fluorescence peaks, from the defined volume element; therefore, a full scan gives rise to a complete diffraction/fluorescence record of the whole sample region of interest. This information record can then be interrogated and interpreted by assembling intensity maps showing the concentration of certain structures (from the diffraction data) or desired atomic elements (from the fluorescence data) within the bulk material system contained in its working environment. This technique can be applied to an enormous variety of materials science situations such as hydrothermal crystallisation of zeolites, hydration/carbonation of cements, processing of industrial materials in model reactors and movement/retention of toxic metals in waste containment systems. For this study it has been necessary to collect *TEDDI* data from the interior of the hydrothermal/autoclave vessel as a function of time; this places great demands on the detector collection rates and so to obtain sufficient time/space resolution the tomographic configuration has been restricted to one-dimensional vertical scanning as indicated in Fig. 2.

The TEDDI measurements described here were all carried out at station 16.4 (energy-dispersive diffraction) at the Synchrotron Radiation Source (SRS), Daresbury Laboratory, UK, this synchrotron operating at a beam energy of 2 GeV and typical beam current of 150–250 mA. Three separate energy-dispersive (Ge solid state) detectors were

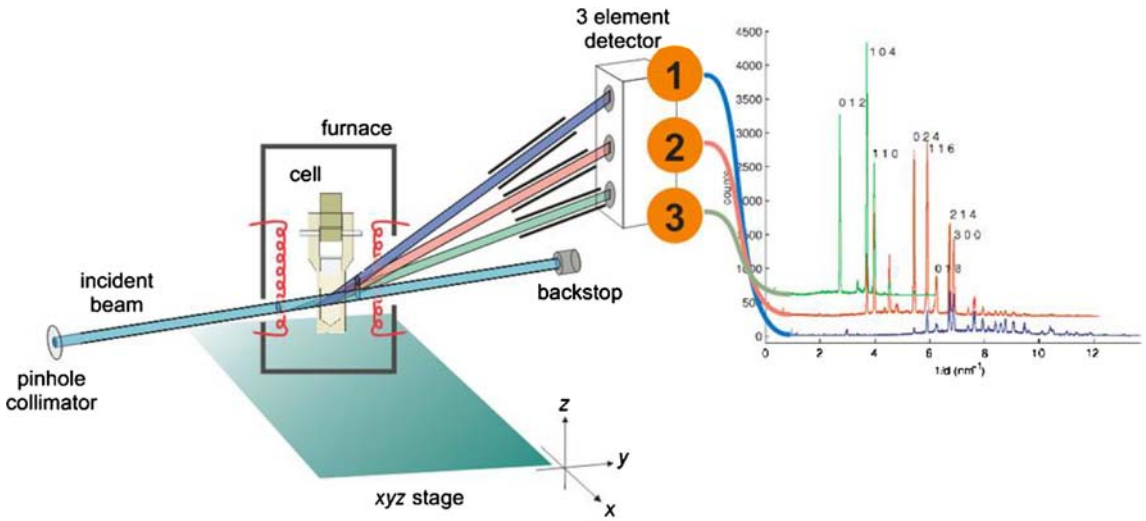

Fig. 1 Schematic diagram of experimental set-up

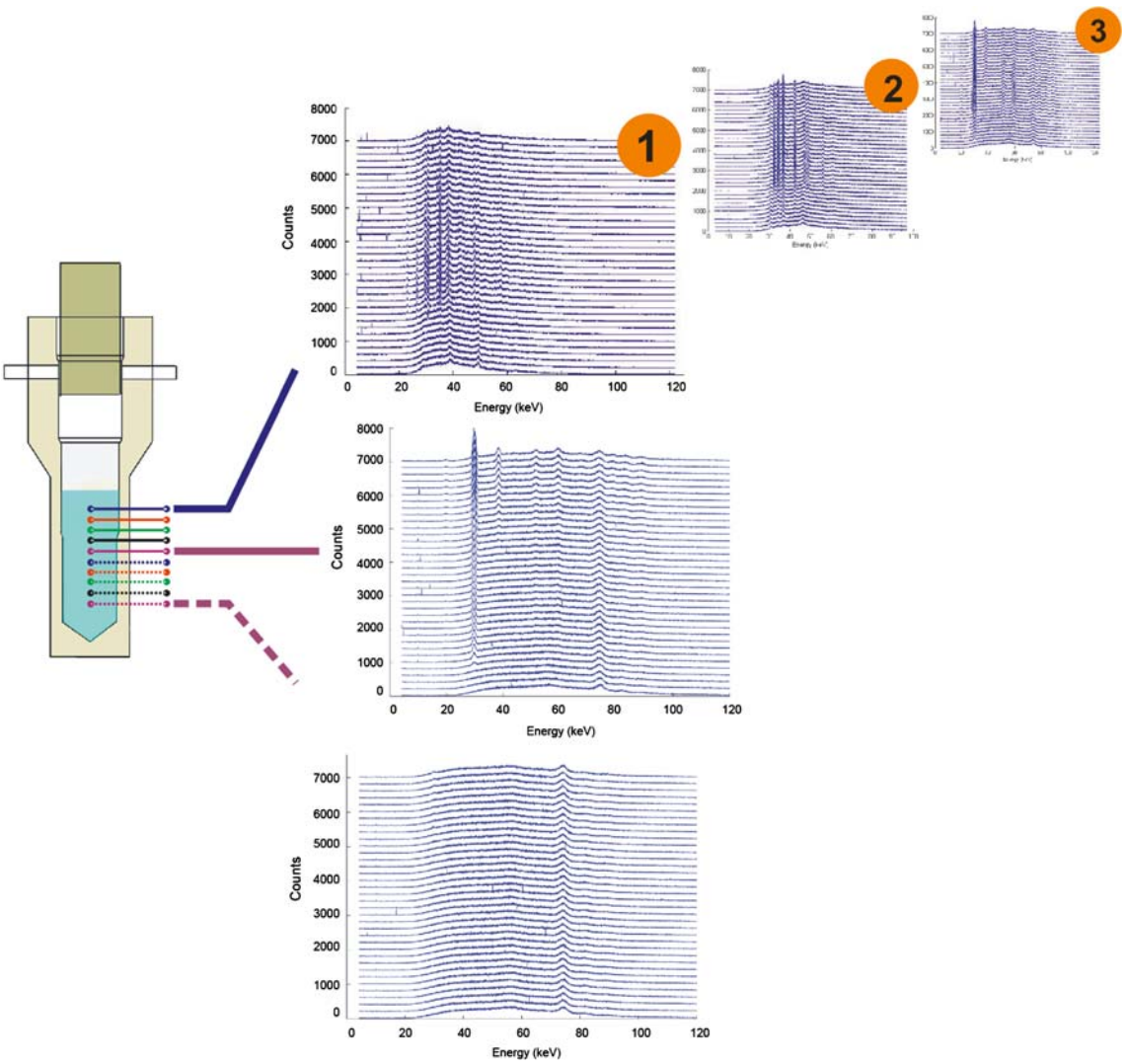

Fig. 2 Schematic illustration of the cell is shown on the left with one-dimensional sampling profile consisting of 10 points. On the right: space/time-resolved energy-dispersive diffraction patterns (intensity versus E) for the top, middle and bottom scan point. For simplicity the data recorded by all three detectors are illustrated only in the case of the top scan point; the collection 2θ angles for the 3 detectors are 2.01°, 4.907° and 7.789°

used (set at 2.01°, 4.907°, 7.789°) which permit three separate diffraction patterns to be collected, each covering different ranges of reciprocal space (*d*-spacing) and therefore also different ranges in X-ray energy. An incident beam cross section of 1 mm diameter was defined using a pinhole collimator. The diffracted beam collimator parameters for three detectors are 0.1 mm each. This defines the discrete diffracting volumes for the three detectors as approximately 0.6, 0.8, and 1.2 mm^3. This setup provides sufficient precision for vertical sampling in steps of 1 mm. Ten such vertical steps are repeatedly cycled throughout the whole synthesis thereby monitoring a vertical range of 9 mm which can be set to reside within the liquid region or across the liquid/vapour interface; the collection time was set at 30 s per step so that each cycle of 10 points took 5 min to complete.

Materials preparation

AlPOs are synthesised from the aluminophosphate reaction mixture in the presence of water-soluble organic templating agents by the conventional hydrothermal method [19]. In a typical synthesis of Ge doped AlPO-5 the following starting materials for the gel were: boehmite powder (36% Al_2O_3) as the source of aluminium, orthophosphoric acid (85% wt) as the source of phosphorus, distilled water, GeO_2 (trigonal form) and triethylamine as the organic

template. The gel was prepared according to the following procedure [20]: 0.694 g boehmite and 3 g distilled water were put into a polypropylene or Teflon beaker. While stirring the starting mixture, 1.15 g orthophosphoric acid was added with, respectively, 0.052 g GeO_2 for 2.5% doping, 0.104 g GeO_2 for 5% doping and 0.208 g GeO_2 for 10% doping. Finally 1.04 g of triethylamine was added to the gel. The final mixture was stirred at ambient temperature (ca. 25 °C) until a homogeneous gel was obtained. The freshly prepared sample was transferred to a PEEK (polyetheretherketone) autoclave cell which resides inside an oven containing suitable X-ray transparent windows [21].

Results

Imaging the hydrothermal environment

Typical examples of space/time-resolved energy-dispersive diffraction patterns are illustrated in Fig. 2 for three representative locations along the vertical axis of the reaction vessel. For each of the 10 locations three sets of EDD patterns were simultaneously collected by the three energy-dispersive detectors (Fig. 2).

A closer look at these plots shown in Fig. 3, reveals the formation of AlPO-5: on the left the diffraction peaks marked at energies 32 keV, 34 keV, 36 keV correspond to the 120, 002, 012 AlPO-5 reflections, respectively, recorded by detector 2. On the right, the stacked plots from detector 3 are showing the AlPO-5 100 reflection and the much weaker AlPO-18 110 reflection.

Effect of % GeO_2-doping

A study was made into the effect of different doping levels of Ge into the AlPO-5 system, the results of which are presented in Fig. 4. Here, a 3 × 3 matrix is shown where the columns correspond to the level of GeO_2 doping (2.5%, 5%, 10%) and the rows represent the 3 observed phases (AlPO-5, GeO_2, AlPO-18). Ten spatially resolved concentration plots are given within each matrix element, coded by colour, and are based on the integrated intensities of the strongest reflections: 100, 112 and 110 for the AlPO-5, GeO_2, AlPO-18 phases, respectively. This matrix is essentially a summary of the events occurring over the vertical axis direction. It suggests that the following takes place in the vessel at the respective levels of GeO_2 doping: an initial period of induction is followed by a period of rapid AlPO-5 crystallisation accompanied by GeO_2 dissolution in the bulk gel (not detected at 2.5% doping). At positions further down the gel, the induction period is seen to increase and the crystallisation rate diminishes, as does the yield. There are spatial variations in the consumption of GeO_2; this is particularly visible in the 10% case where there is a smaller fraction of GeO_2 consumed overall, and the extent of consumption correlates with AlPO-5 yield.

At 2.5% doping, it is evident that AlPO-5 crystallises at two stages, at least in the upper half of the scanned region. In the first stage, formation of AlPO-5 proceeds in a manner similar to that of 5% and 10% doping, with similar trends in induction and crystallisation rate and indeed yield. At the top of the vessel, following a second induction period, a second AlPO-5 crystallisation event occurs; again, the rate diminishes and the induction period

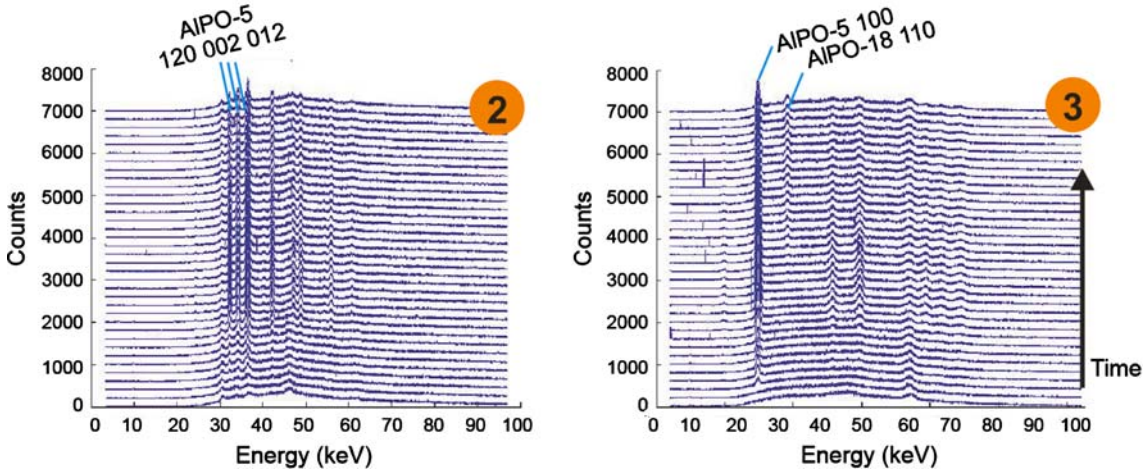

Fig. 3 Typical examples of space/time-resolved energy-dispersive diffraction patterns collected during the crystallisation of 2.5% Ge doped AlPO-5 at 170 °C. Stacked diffraction plots on the left, recorded by detector 2, show three strong reflections 120, 002, 012, associated with AlPO-5 structure. On the right, recorded by detector 3, the AlPO-5 reflection 100 is denoted together with a much weaker reflection related to AlPO-18 phase

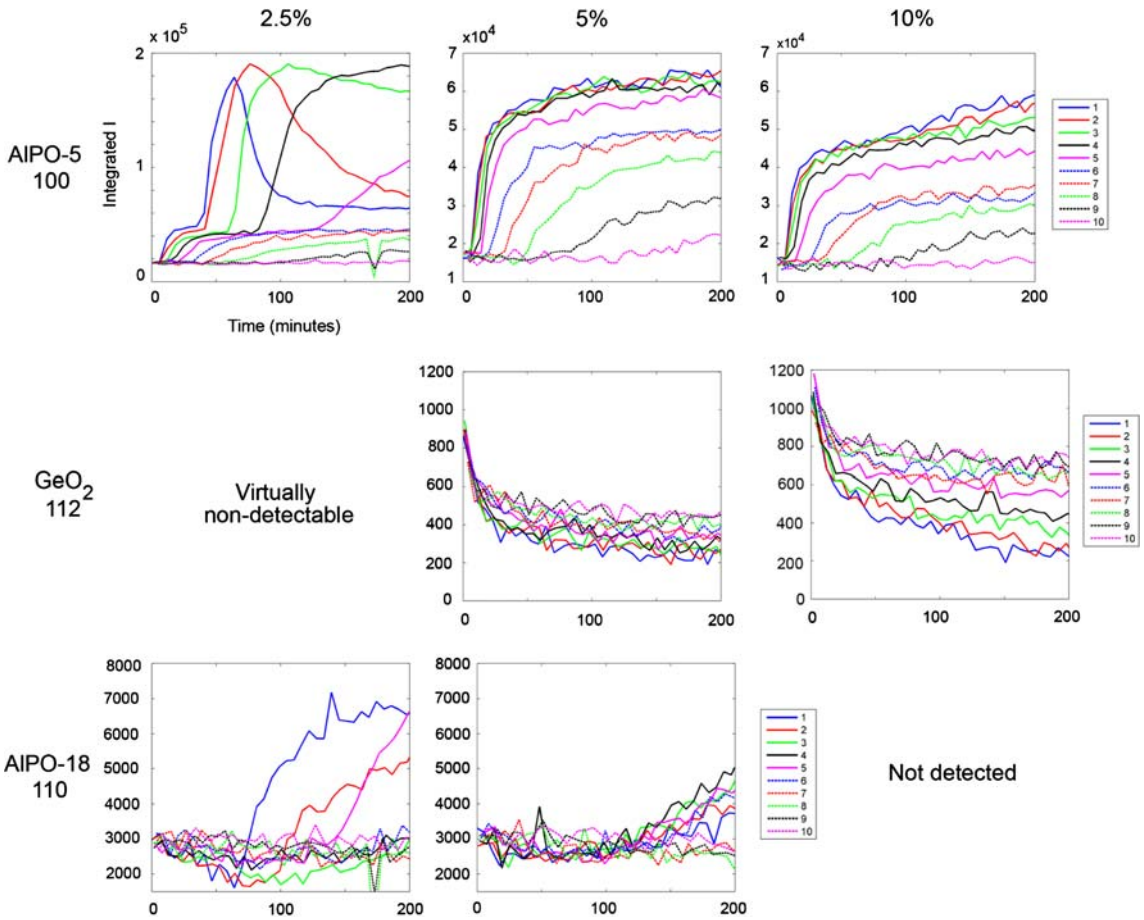

Fig. 4 Summarised concentration plots obtained from the integrated intensities of reflections 100, 112 and 110 for the AlPO-5, GeO_2, AlPO-18 phases, respectively, at 10 scan points within the hydrothermal vessel as described in the main body of the text

lengthens moving down the gel. This newly formed AlPO-5 goes on to decompose and form a phase identified as AlPO-18. It can be seen that the yield and rate of conversion of AlPO-5 to AlPO-18 increases towards the top of the scan and hence closer to the top of the gel. The AlPO-18 phase is also observed in the 5% doped gel but is undetectable in the 10% case.

The gel–vapour interface

In order to explore sampling points higher up in the vessel, an additional configuration was used in which the 10 scan points were positioned to cover the gel–vapour interface during the 2.5% Ge doped AlPO-5 crystallisation. Figure 5 compares these 10 scan points (AlPO-5 concentration curves in left graphic) to the ones used in the previous experiment (shown in the right graphic of Fig. 5 and in the upper left graphic of Fig. 4) where all scan points were positioned within the gel. The concentration curves indicate a shorter induction period (differences in induction are negligible at, and very close to, the surface) and higher crystallisation rate closer to the gel–vapour interface although this is not reflected in the yield; these trends match those described in the section above.

Discussion and conclusions

This study shows that very significant variation in synthesis pathway and kinetics can occur during hydrothermal/autoclave synthesis, in this case of a prototype aluminophosphate microporous material, AlPO-5. The possible causes for this will be a combination of factors such as:

- preferential nucleation and early crystallisation towards the liquid/gas interface;
- settling under gravity (downward vertical movement) of the crystallites through the liquid phase;
- small temperature gradients across the autoclave vessel;
- convection currents induced by the above factors and as previously implicated by Hooper [22];

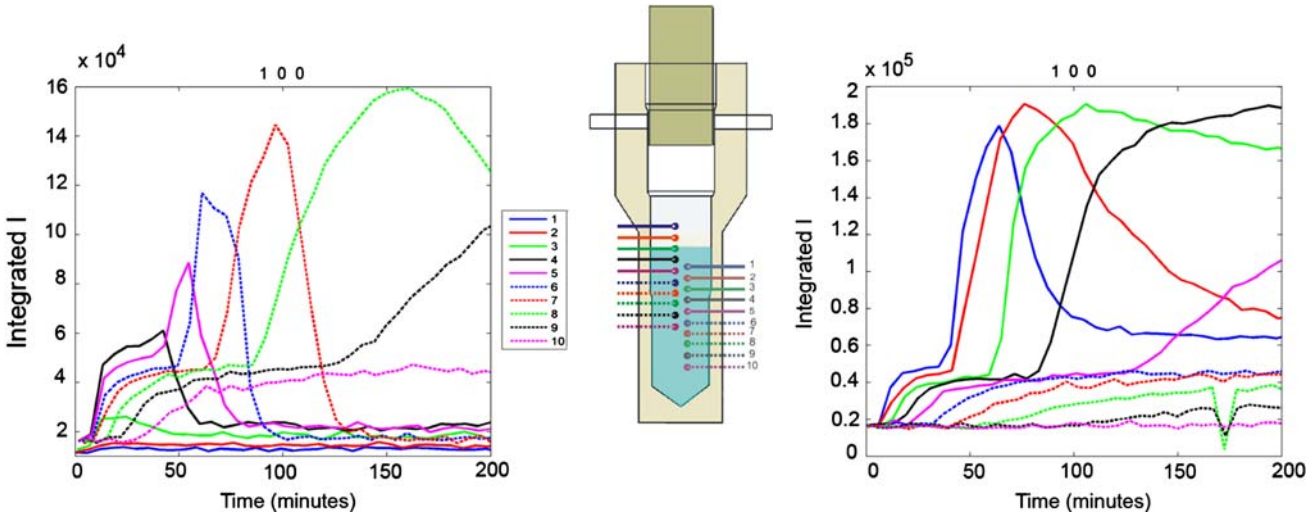

Fig. 5 Representative concentration plots, both of 2.5% GeO_2 doped AlPO-5, obtained in two separate experiments, showing the strongest AlPO-5 100 reflection: on the left, points 1–4 span the interface zone with point 3 being the most likely scan point at the boundary of the gel–vapour interface

- a stage where the desired product (ALPO-5) acts as an intermediate to a secondary (ALPO-18) product.

That fact that TEDDI can observe such large variations in synthesis pathway throws a double challenge: to the tomography field to fully understand the origins of these crystallisation gradients and to the larger synthesis/in situ diffraction community to question the validity of the in situ results obtained to date. It must be emphasised that these differences amount to more than small variation in kinetics; the differences are large and different pathways are evident: For example, if an experimenter were to study the same sequence reported here, very different conclusions could have been arrived at depending on the vertical positioning of the X-ray analysis point within the autoclave vessel; one pathway observed would be a direct crystallisation of ALPO-5 whereas the other would point to ALPO-5 acting as an intermediate towards producing the ALPO-18 phase; it may not be coincidental that the presence of ALPO-18 during synthesis has been observed previously by others [17, 23–25]. In conclusion, it follows that a TEDDI description of the total vessel gives a fuller picture of the whole synthesis and that such information should eventually be exploited in the design of such hydrothermal cells so that they are optimised specifically for production of a given phase.

Acknowledgements The authors would like to gratefully acknowledge the EPSRC for financial support, the Daresbury Laboratory (SRS) for the award of synchrotron beamtime, and Prof Gopinathan Sankar for valuable comments.

References

1. Polak E, Munn J, Barnes P, Tarling SE, Ritter C (1990) J Appl Cryst 23:258
2. Munn J, Barnes P, Hausermann D, Axon SA, Klinowski J (1992) Phase Transit 39:129
3. He H, Barnes P, Munn J, Turrillas X, Klinowski J (1992) Chem Phys Lett 196:267
4. Fogg AM, Price SJ, Francis RJ, O'Brein S, O'Hare D (2000) J Mater Chem 10:2355
5. Davies AT, Sankar G, Catlow CRA, Clark SM (1997) J Phys Chem B 101:10115
6. Beale AM, Sankar G (2003) Chem Mater 15:146
7. Norby P, Christensen AN, Hanson JC (1999) Inorg Chem 38:1216
8. Norby P (2006) Curr Opin Colloid Interface Sci 11:118
9. Hooper D, Barnes P, Cockcroft JK, Jupe AC, Jacques SDM, Bailey SP, Lupo F, Vickers M, Hanfland M (2003) Phys Chem Chem Phys 5:4946
10. Hall C, Barnes P, Cockcroft JK, Colston SL, Hausermann D, Jacques SDM, Jupe AC, Kunz M (1998) Nucl Instrum Meth Phys Res B 140:253
11. Barnes P, Jupe AC, Jacques SDM, Colston SL, Cockcroft JK, Hooper D, Betson M, Hall C, Barè S, Rennie AR, Shannahan J, Carter MA, Hoff WD, Wilson MA, Phillipson MC (2001) Nondestr Test Eval 17:143
12. Caro J, Marlow F, Hoffmann K, Striebel C, Kornatowski J, Girnus I, Noack M, Kölsch P (1997) Stud Surf Sci Catal 105:2171
13. Li ZM, Liu HJ, Ye JT, Chan CT, Tang ZK (2004) Appl Phys A 78:1121
14. Davies AT, Sankar G, Catlow CRA, Clark SM (1997) J Phys Chem B 101:10115
15. Muncaster G, Davies AT, Sankar G, Catlow CRA, Thomas JM, Colston SL, Barnes P, Walton RI, O'Hare D (2000) Phys Chem Chem Phys 2:3523
16. Pastore HO, Coluccia S, Marchese L (2005) Annu Rev Mater Res 35:351

17. Huang Y, Demko BA, Kirby CW (2003) Chem Mater 15:2437
18. Betson M, Barker J, Barnes P, Atkinson T, Cockcroft JK (2004) Transport Porous Media 57:203
19. Wilson ST, Lok BM, Messina CA, Cannan TR, Flanigen EM (1982) J Am Chem Soc 104:1146
20. Chen J, Sankar G, Thomas JM, Xu R, Greaves GN, Waller D (1992) Chem Mater 4:1373
21. Lupo F, Cockcroft JK, Barnes P, Stukas P, Vickers M, Norman C, Bradshaw H (2004) Phys Chem Chem Phys 6:1837
22. Hooper D (2004) Time and space resolved analysis of chemical and material systems. Ph.D. Thesis, University of London
23. Davies AT, Sankar G, Catlow CRA, Clark SM (1997) J Phys Chem B 101:10115
24. Muncaster G, Davies AT, Sankar G, Catlow CRA, Thomas JM, Colston SL, Barnes P, Walton RI, O'Hare D (2000) Phys Chem Chem Phys 2:3523
25. Pastore HO, Coluccia S, Marchese L (2005) Annu Rev Mater Res 35:351